

Insulin-like growth factor 2 mRNA-binding protein 2 is a therapeutic target in ovarian cancer

Jia Yuan^{1,2}, Xin Li^{1,2}, Fanchen Wang^{1,2}, Huiqiang Liu^{1,2}, Wencai Guan¹ and Guoxiong Xu^{1,2,3} 

¹Research Center for Clinical Medicine, Jinshan Hospital, Fudan University, 1508 Longhang Road, Shanghai 201508, China;

²Department of Oncology, Shanghai Medical College, Fudan University, Shanghai 200032, China; ³Center for Tumor Diagnosis and Therapy, Jinshan Hospital, Fudan University, Shanghai 201508, China

Corresponding author: Guoxiong Xu. Email: guoxiong.xu@fudan.edu.cn

Impact Statement

Ovarian cancer (OC) is a fatal gynecologic disease and is often resistant to chemotherapy. IGF2BP2 is an oncogene but little is known about its role in paclitaxel resistance and the clinical prognosis of OC. This study identifies and characterizes IGF2BP2 as a potential therapeutic target and diagnostic biomarker for OC. It explores for the first time the responsibility and function of IGF2BP2 in OC. The outcomes obtained in the study substantiate that IGF2BP2 is associated with prognosis and can be an indicator for immunotherapy in chemoresistant patients.

Abstract

Ovarian cancer (OC) is a fatal gynecologic disease. The most common treatment for OC patients is surgery combined with chemotherapy but most patients at advanced stages eventually develop relapse due to chemoresistance. This study examined the role and function of insulin-like growth factor 2 mRNA-binding protein 2 (IGF2BP2) in OC. We observed that the expression of IGF2BP2 mRNA and protein was up-regulated in OC cells and tissues using quantitative real-time polymerase chain reaction (qRT-PCR) and western blot, respectively. An increase in IGF2BP2 expression at mRNA and protein levels was verified by the analyses of The Cancer Genome Atlas (TCGA) and Clinical Proteomic Tumor Analysis Consortium (CPTAC), respectively. Gene Expression Omnibus (GEO) and Cancer Cell Line Encyclopedia (CCLE) databases were applied to analyze the expression and clinical value of IGF2BP2. Gene set enrichment analysis (GSEA), Kyoto Encyclopedia of Genes and Genomes (KEGG), and Gene Ontology (GO) analyses explored biological functions and the involvement of IGF2BP2 in cell growth. Indeed, the knockdown

of IGF2BP2 resulted in the inhibition of OC cell proliferation evaluated by the Cell Counting Kit-8 assay. Genomic amplification of IGF2BP2 partly accounted for its overexpression. High expression of IGF2BP2 was associated with signal transducer and activator of transcription 1 (STAT1) and drug sensitivity and was correlated with an unfavorable survival outcome in OC patients. Furthermore, the responsiveness of chemotherapy and immunotherapy were analyzed using the “pRRophetic” R package and The Cancer Immune Atlas (TCIA) database, respectively. The low expression of IGF2BP2 was associated with chemoresistance but with high tumor microenvironment scores and tumor-infiltrating immune cells, suggesting that immunotherapy may apply in chemoresistant patients. The alteration of IGF2BP2 expression may respond to chemotherapy and immunotherapy. Thus, IGF2BP2 shows potential as a therapeutic target and diagnostic biomarker for OC.

Keywords: Chemotherapy, drug resistance, immune, ovarian tumor, prognosis, STAT1

Experimental Biology and Medicine 2023; 248: 2198–2209. DOI: 10.1177/15353702231214268

Introduction

Ovarian cancer (OC) is a fatal gynecologic disease.¹ Due to the insidious onset and rapid progression, about 70% of patients suffer from advanced OC and only 20–30% of patients at advanced stages survive for more than five years.² The most common treatment for OC is surgical treatment combined with paclitaxel (PTX) and platinum-based chemotherapy. More than 80% of OC patients initially respond to anticancer drugs but most of them eventually develop relapse because of resistance to chemotherapy.³ Therefore,

it needs to identify promising biomarkers for therapeutic intervention and prognostic prediction in OC.

Insulin-like growth factor 2 mRNA-binding protein 2 (IGF2BP2, also known as IMP2) is involved in the localization, stability, and translation of RNAs⁴ and plays a crucial role in the occurrence and development of tumors.⁵ Study has shown that IGF2BP2 up-regulation predicts shortened overall survival (OS) of pancreatic cancer patients.⁶ However, there is limited knowledge regarding the biological function, molecule mechanism, and therapeutic value of IGF2BP2 in OC.⁷ Our previous study showed that STAT1

was overexpressed in OC and stimulated cell proliferation, migration, and invasion.⁸ Besides, we also observed that STAT1 mRNA and protein expression was down-regulated in PTX-resistant OC cell lines and was with excessive methylation of CpG in the promoter region.⁹ The mechanism of differentially expressed STAT1 between PTX-sensitive and PTX-resistant cells is unknown. We speculated that the post-transcriptional modification may have a significant impact on the differential expression of STAT1. N6-methyladenosine (m⁶A) methylation is a common post-transcriptional RNA modification in epigenetic regulations and exhibits significant associations with the progression of malignant tumors.¹⁰ Referring to the bioinformatics prediction, IGF2BP2 is a potential m⁶A “reader” that binds to STAT1 and regulates STAT1 expression. Furthermore, our previous work also showed that STAT1 was closely related to the immune microenvironment of tumorigenesis, and STAT1 overexpression was positively associated with up-regulated programmed death-1 (PD-1) and PD-ligand 1 (PD-L1) in OC.¹¹ Nevertheless, the relationship between IGF2BP2 and STAT1, tumor immune, and chemoresistance remains unclear.

In this study, we explored the oncogenic role and characteristics of IGF2BP2 in OC. The association of IGF2BP2 with STAT1 was conducted as well. Moreover, the multidatabase analyses of genetic alterations, prognosis, reactive sensitivity of chemotherapy and immunotherapy, and tumor-infiltrating cells with different levels of IGF2BP2 expression were also elucidated.

Materials and methods

Cell culture and transfection

All utilized cells were human-derived cells and authenticated using short tandem repeat (STR) analysis. Non-tumorous human immortalized ovarian surface epithelial cells (IOSE-80) (ScienCell, Shanghai, China), ovarian endometrioid adenocarcinoma cells originally derived from the tumor tissue (A2780) (Keygen Biotech, Nanjing, Jiangsu, China), and paired PTX-resistant cells (A2780-PTX) (Keygen Biotech) were grown in Dulbecco's modified eagle medium (Gibco, Invitrogen, Carlsbad, CA, USA) supplemented with 10% fetal bovine serum (FBS, Invitrogen). Ovarian serous adenocarcinoma cells originally derived from the ascites (OVCAR-3) and paired PTX-resistant cells (OV3R-PTX)⁹ were grown in RPMI-1640 medium (Gibco) supplemented with 20% FBS. Ovarian serous cystadenocarcinoma cells originally derived from the ascites (SK-OV-3) and paired PTX-resistant cells (SK3R-PTX)¹² were grown in McCoy's 5A medium (Gibco) supplemented with 10% FBS. Cells were transfected with IGF2BP2-small interfering RNA (siRNA) or negative control (NC)-siRNA synthesized by Shanghai GenePharma Co., Ltd (Shanghai, China) using X-tremeGENE siRNA Transfection Reagent (Roche Applied Science, Indianapolis, IN, USA). The sequences of siRNA (si-NC, si-IGF2BP2-1, and si-IGF2BP2-2) are shown in Supplementary Table S1. The IGF2BP2-overexpressing plasmid was constructed by inserting a coding sequence (CDS) of the *IGF2BP2* gene at positions 83-1882 (GenBank Accession #: NM_006548.6) into the pCMV vector (Miaoling Biology, Wuhan, Hubei, China). Cells were seeded

into a six-well plate and transfected with 2.5 µg/well plasmid using Lipo8000 (Beyotime Biotechnology, Shanghai, China). RNA and protein samples were obtained after 24 and 48 h transfection.

Cell viability detection

NC and IGF2BP2-siRNA-expressed cells (SK-OV-3 and A2780) were plated in a 96-well plate with a density of 3×10^3 /well and grown for 24, 48, and 72 h. The cell viability was evaluated using the Cell Counting Kit-8 (CCK-8, Dojindo Laboratories, Kumamoto, Japan) kit. The relative cell number was calculated using the formula: Relative cell number = $(T_{OD450nm} - \Delta B_{OD450nm}) / (\Delta 0hT - C_{OD450nm}) \times 100\%$. $T_{OD450nm}$ indicates the absorbance value at optical density (OD) 450 nm in the tested cells at 0, 24, 48, or 72 h. $\Delta B_{OD450nm}$ indicates the average of the absorbance value at OD450 nm in the blank without cells at 0, 24, 48, or 72 h. $\Delta 0hT - C_{OD450nm}$ indicates the average value of the tested cells minus the blank without cells at 0 h.

Quantitative real-time polymerase chain reaction

The RNA-Quick Purification Kit (Yishan Biotechnology Co., Ltd, Shanghai, China) and the qPCR RT Kit (Mei5 Biotechnology Co., Ltd, Beijing, China) were utilized to extract total RNA and to perform polymerase chain reaction (PCR), respectively, according to the manufacturer's instructions. The sequences of PCR primer are shown in Supplementary Table S2. To ensure reliability, the levels of target gene expression were normalized to β -actin. To determine the threshold cycle (Ct), the 7300 real-time PCR system (V1.4, Applied Biosystems, Waltham, MA, USA) was utilized.

Protein extraction and western blot analysis

Cell lysates were obtained after ultrasonic cracking with a lysis buffer containing sodium dodecyl sulfate (SDS), benzyl sulfonyl fluoride, and phosphatase inhibitors. Protein samples were run in SDS-polyacrylamide gel electrophoresis. The primary antibody of the rabbit anti-IGF2BP2 (1:1000 dilution) was obtained from Proteintech (Wuhan, China); rabbit anti-STAT1 (1:1000 dilution) was obtained from Cell Signaling Technology, Inc. (Danvers, MA, USA); mouse anti- β -actin (1:5000 dilution), and the secondary antibodies of goat antirabbit IgG and antimouse IgG labeled with horseradish peroxidase (both 1:5000 dilution) were obtained from Proteintech. The signals were detected by the chemiluminescence imaging system (Tanon Science & Technology, Shanghai, China). The relative optical density of protein bands was semi-quantified using ImageJ 1.6.0 (<https://imagej.nih.gov/ij/>).

Data acquisition

Transcriptome RNA-sequencing data of OC were obtained from the databases of The Cancer Genome Atlas (TCGA) (<https://portal.gdc.cancer.gov/>) and the University of California-Santa Cruz Xena Browser (<https://xena.ucsc.edu/>) combined with normal ovary tissues from the Genotype-Tissue Expression (GTEx) database (

xenabrowser.net/datapages/). Data from OC and normal ovarian samples were extracted from the Gene Expression Omnibus (GEO) (<https://www.ncbi.nlm.nih.gov/geo/>), including gene set enrichment (GSE)12470, GSE14407, GSE18520, GSE26712, GSE38666, and GSE40595 data sets. The selection criteria for the GSE series were based on searching keywords that included OC, tumor subtype, expression profiling by array, and homo sapiens. The exclusive criteria were as follows: patients without additional treatment such as chemotherapy, lack of normal control, the knockdown of a gene, and case number less than 6 in a group. The protein data were obtained from the Clinical Proteomic Tumor Analysis Consortium (CPTAC) (<http://ualcan.path.uab.edu/analysis-prot.html>).

Prognostic value analysis

The prognostic value of IGF2BP2 was analyzed using Kaplan–Meier plotter (<http://kmplot.com/analysis/>) for OS and progression-free survival (PFS). The survival analysis of patients with IGF2BP2 expression in GEO data sets was performed by Prognoscan (<http://dna00.bio.kyutech.ac.jp/Prognoscan/>)¹³ using the selection criteria by searching keywords IGF2BP2 and OC. Case numbers less than 6 for each group and the probe ID other than #223963 were excluded. The UALCAN online tool (<http://ualcan.path.uab.edu/index.html>)¹⁴ was employed to examine the association of IGF2BP2 expression with clinical characteristics such as different stages and ages of OC patients. The effectiveness of a diagnostic IGF2BP2 and the selection of an optimal threshold value (cutoff point) for IGF2BP2 were measured by the Youden index (the Youden index = Sensitivity + Specificity – 1).¹⁵ The “pROC” and “ggplot2” R packages (<https://www.bioconductor.org/>) were used to plot the receiver operating characteristic (ROC) curve.

cBioPortal database analysis

An open-access cBioPortal (<https://www.cbioportal.org/>)¹⁶ which incorporates multiple genomic data types from TCGA was used for analyzing somatic mutations and DNA copy-number alterations (CNAs) of IGF2BP2.

Cancer Cell Line Encyclopedia

The multiomics maps of OC cell lines and information on genetic mutations, DNA methylation, RNA splicing, and histone modification were extracted from the RNA-seq database of the Cancer Cell Line Encyclopedia (CCLE) (<https://sites.broadinstitute.org/ccle/>). Gene sets significantly correlated with IGF2BP2 expression were screened out. The enrichment analyses were performed using the Kyoto Encyclopedia of Genes and Genomes (KEGG) and Gene Ontology (GO) using R software (version 4.1.3).

Gene Set Enrichment Analysis

To clarify the activity of related functions and signal pathways in OC between the IGF2BP2-high and IGF2BP2-low groups (IGF2BP2^{high} versus IGF2BP2^{low}), KEGG gene set files in Gene set enrichment analysis (GSEA) (<https://www.gsea-msigdb.org/gsea/index.jsp>) were downloaded

and analyzed by GSEA 4.1.0 in OC samples. Multiple GSEA plots were performed through “plyr,” “ggplot2,” “grid,” and “gridExtra” R packages.

IGF2BP2 prediction in drug sensitivity

The “pRRophetic” R package (<http://genemed.uchicago.edu/~pgeeheher/pRRophetic/>)¹⁷ was used to measure the difference in the half-maximal inhibitory concentration (IC₅₀) between the IGF2BP2-high and IGF2BP2-low groups from TCGA-OV.

Tumor microenvironment and immune cell infiltration analysis

The tumor microenvironment (TME) of OC was scored by the ESTIMATE R package.¹⁸ The three final scores: stromal score, immune score, and ESTIMATE score were generated. The CIBERSORT algorithm generally deconvolutes the tumor tissue expression matrix by using the linear support vector regression method to analyze the content of various types of cells in the tissue.¹⁹ Therefore, this algorithm was utilized to obtain the related content of immune cells in TCGA-OC. The results of immune cell infiltration in each sample and the expression of IGF2BP2 in OC were analyzed.

Immunotherapy analysis

The immunotherapy scoring file of OC was downloaded from The Cancer Immunome Atlas (TCIA) database (www.cancerimagingarchive.net), including two classical immune checkpoints: cytotoxic T-lymphocyte-associated protein 4 (CTLA4) and PD-1. Immunotherapy scoring files from TCIA and IGF2BP2 expression files from TCGA-OV were integrated for immunotherapy analysis by “limma” and “ggpubr” R packages.

Statistical analysis

All statistical analyses were conducted utilizing GraphPad Prism 8.0 (<https://www.graphpad.com/>). Statistical significance was assessed by the unpaired two-tailed Student’s *t*-test or one-way analysis of variance (ANOVA). Results with *P* < 0.05 were considered statistically significant.

Results

IGF2BP2 is overexpressed in OC

The levels of IGF2BP2 mRNA and protein expression were higher in OC cells (OVCAR-3, SK-OV-3, and A2780) compared with non-tumorous IOSE-80 cells (Figure 1(A) to (C)) detected by quantitative real-time PCR (qRT-PCR) (*n* = 3) and western blot (*n* = 3), respectively. The analyzed data from GSE12470, GSE14407, GSE18520, GSE26712, GSE38666, and GSE40595 data sets also supported the fact that the level of IGF2BP2 mRNA expression was significantly elevated in OC tissues compared with normal ovarian tissues (Figure 1(D) to (I)). By combining the RNA-seq data from TCGA and GTEx databases, we found that the levels of IGF2BP2 mRNA expression were also high in OC tissues compared with normal tissues (Figure 1(J)). Furthermore, data analysis

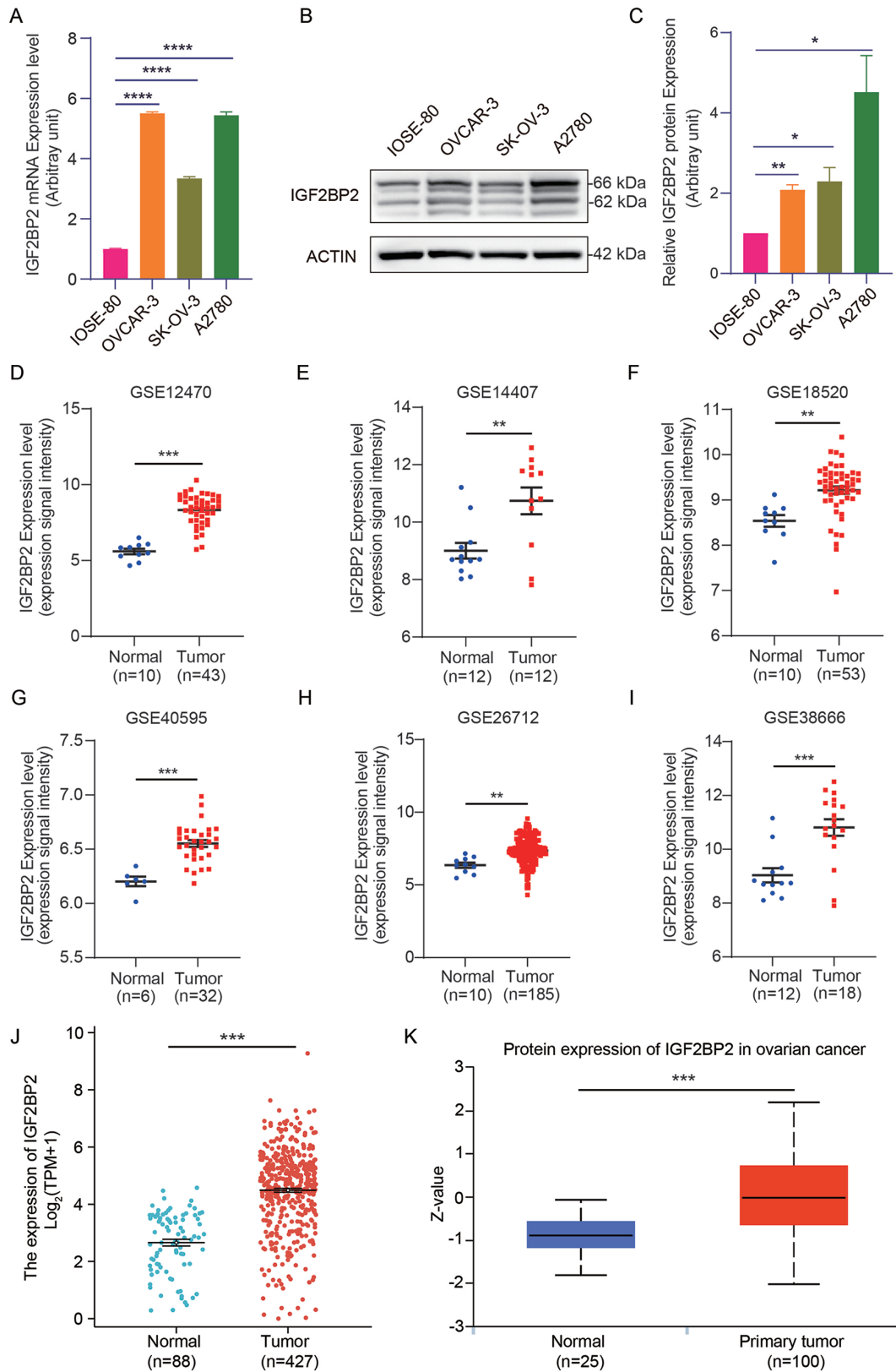


Figure 1. IGF2BP2 expression in OC cells and tissues: (A) the expression of IGF2BP2 mRNA was detected by quantitative real-time polymerase chain reaction in OC cells (OVCAR-3, SK-OV-3, and A2780) and non-tumorous IOSE-80 cells, and the experiment was repeated three times; (B) the expression of IGF2BP2 protein was detected by western blot in OC cells and IOSE-80 cells, and representative images of IGF2BP2 and ACTIN are shown ($n=3$); (C) semi-quantitative analysis of the relative optical density of protein bands from B ($n=3$); (D to I) the expression level of IGF2BP2 mRNA was elevated in OC tissues (tumor) compared with normal ovarian tissues (normal) from Gene Expression Omnibus data sets (GSE12470, GSE14407, GSE18520, GSE26712, GSE38666, and GSE40595); (J) the expression level of IGF2BP2 mRNA in OC tissues (tumor) and normal ovarian tissues (normal) from The Cancer Genome Atlas-OV; (K) the expression of IGF2BP2 protein in OC tissues (tumor) and normal ovarian tissues (normal) from Clinical Proteomic Tumor Analysis Consortium-OV. OC: ovarian cancer; IGF2BP2: insulin-like growth factor 2 mRNA-binding protein 2; IOSE: immortalized ovarian surface epithelial cells; GSE: gene set enrichment. * $P < 0.05$; ** $P < 0.01$; *** $P < 0.001$; **** $P < 0.0001$.

from the CPTAC database revealed a significant increase in IGF2BP2 protein in OV primary tumors compared with normal samples (Figure 1(K)).

Knockdown of IGF2BP2 inhibits cell proliferation in OC

The analyses of the RNA-seq data of 47 OC cell lines derived from CCLE showed that there were 76 genes significantly associated with IGF2BP2 expression by the correlation test ($P < 0.001$ with $\text{corFilter} > 0.5$). KEGG pathway enrichment analysis exhibited that IGF2BP2 positively or negatively correlated genes gathered at the pathways regarding the process of DNA duplication and cell cycle, such as “mitotic cell cycle phase transition,” “signal transduction by p53 class mediator,” and “mitotic G2 DNA damage checkpoint signaling” (Figure 2(A)). The results of GO term analyses, including biological process (BP), cellular component (CC), and molecular function (MF) categories, disclosed that IGF2BP2-coexpressed genes were also involved in the “mitotic cell cycle transition,” “methyltransferase complex,” “translation regulator activity,” and “catalytic activity, acting on DNA” (Figure 2(B)). In addition, GSEA in OC from CCLE revealed that the up-regulated genes with high IGF2BP2 expression were enriched in cell cycle, DNA replication, and Fc γ R-mediated phagocytosis, whereas the down-regulated genes were gathered in ATP-binding cassette (ABC) transporters, drug metabolism, and complement and coagulation cascades (Figure 2(C)). Based on the above analyses, we conducted the CCK-8 assay to evaluate the influence of IGF2BP2 on OC cell proliferation. The inhibition of cell proliferation was observed upon IGF2BP2 knockdown in SK-OV-3 and A2780 cells (Figure 2(D)).

IGF2BP2 gene is amplified in OC

The cBioPortal online tool was utilized to figure out the close-up view of IGF2BP2 alteration frequency in pan-cancer. Amplification was found to be responsible for most genomic alterations in cancers, including OC (OV at the second position) (Figure 3(A)). Further analysis of the DNA-seq data disclosed that the IGF2BP2 gene was altered in 105 of 585 cases of OC (18%) and these alterations were amplified (Figure 3(B)). Further analyses revealed that IGF2BP2 protein expression was high in the chromatin modifier altered group ($n = 66$) and a group of others including DNA gene copy number variations and gene mutation ($n = 13$) compared with the normal group ($n = 25$) (Figure 3(C)). Next, we found that patients with IGF2BP2 alterations had shorter OS compared with patients with unaltered IGF2BP2 based on the TCGA pan-cancer data sets (Figure 3(D)).

High-expressed IGF2BP2 is associated with poor prognosis and survival of OC patients

Additional survival analyses revealed that OC patients with high-expressed IGF2BP2 tended to have shorter OS and PFS compared with those with low-expressed IGF2BP2 detected by the Kaplan–Meier plotter (Figure 4(A) and (B)). Furthermore, patients with up-regulated IGF2BP2 were unfavorable to the OS found in the GSE9891 data set (Figure 4(C)) using PrognScan. By analyzing CPTAC samples of OC, a

positive correlation between the expression of IGF2BP2 protein and the tumor Stage 3 and more than 41 years of patients was observed (Figure 4(D) and (E)). The accuracy of the prediction of the patient outcomes was estimated using the ROC curve. The true positive rate (TPR) and the false positive rate (FPR) were 0.712 (sensitivity) and 0.955 (specificity), respectively, when the optimal cutoff value of IGF2BP2 was 3.960 (the maximum value of the Youden index) (Figure 4(F)). The high area under the curve (AUC) value (0.852) demonstrated that IGF2BP2 as a biomarker had high accuracy in predicting the patient outcomes.

Expression of IGF2BP2 is positively correlated with STAT1 expression and chemoresistance

The IGF2BP2 mRNA and protein expression was lower in PTX-resistant OC cells (OV3R-PTX, SK3R-PTX, and A2780-PTX) than in their counterpart-sensitive cells (OVCAR-3, SK-OV-3, and A2780) (Figure 5(A) to (C)). Coincidentally, the down-regulation of STAT1 mRNA and protein expression in PTX-resistant OC cells were also observed (Figure 5(D) to (F)). With the inhibition of IGF2BP2 using two specific siRNA (si-IGF2BP2-1 and si-IGF2BP2-2), the expression of STAT1 was decreased at mRNA and protein levels synchronously in SK-OV-3 and A2780 cells (Figure 5(G) and (H)). Overexpression of IGF2BP2 led to an increase in STAT1 mRNA and protein expression (Supplementary Figure S1). Next, we analyzed the correlation of IGF2BP2 expression with the sensitivity of nine anticancer drugs, including AZD.0530, bleomycin, cisplatin, docetaxel, doxorubicin, etoposide, gemcitabine, pazopanib, and vinorelbine. The high IC₅₀ values were observed in the IGF2BP2 low-expression group compared with the high-expression group (Supplementary Figure S2), indicating that OC patients with low expression of IGF2BP2 tend to be less sensitive to these anticancer drugs.

IGF2BP2 expression is associated with the TME and sensitivity to immunotherapy

It has been shown that the TME exerts a significant influence on tumor progression and therapeutic response. GSEA showed that IGF2BP2 was associated with immune-related pathways. By assessing TMEs from TCGA-OV using the ESTIMATE algorithm, low IGF2BP2 expression was associated with high scores of stroma, immune, and ESTIMATE compared with high IGF2BP2 expression (Figure 6(A)). Further CIBERSORT analysis showed that six types of tumor-infiltrating immune cells (TICs), including B-cell naive ($P = 0.012$), natural killer (NK) cells activated ($P = 0.042$), NK cells resting ($P = 0.034$), B-cell memory ($P = 0.033$), neutrophils ($P = 0.030$), and mast cells activated ($P = 0.016$) were significantly correlated with IGF2BP2 expression (Figure 6(B); Supplementary Figure S3). Immunotherapeutic sensitivity analysis displayed that OC patients with the low expression of IGF2BP2 had high immune scores (Figure 6(C) to (F)), indicating that those patients may increase their sensitivity to the immunotherapy no matter the negative or positive of CTLA4 and PD-1 and suggesting that immunotherapy can be used in patients with the resistance of chemotherapy and low-expressed IGF2BP2.

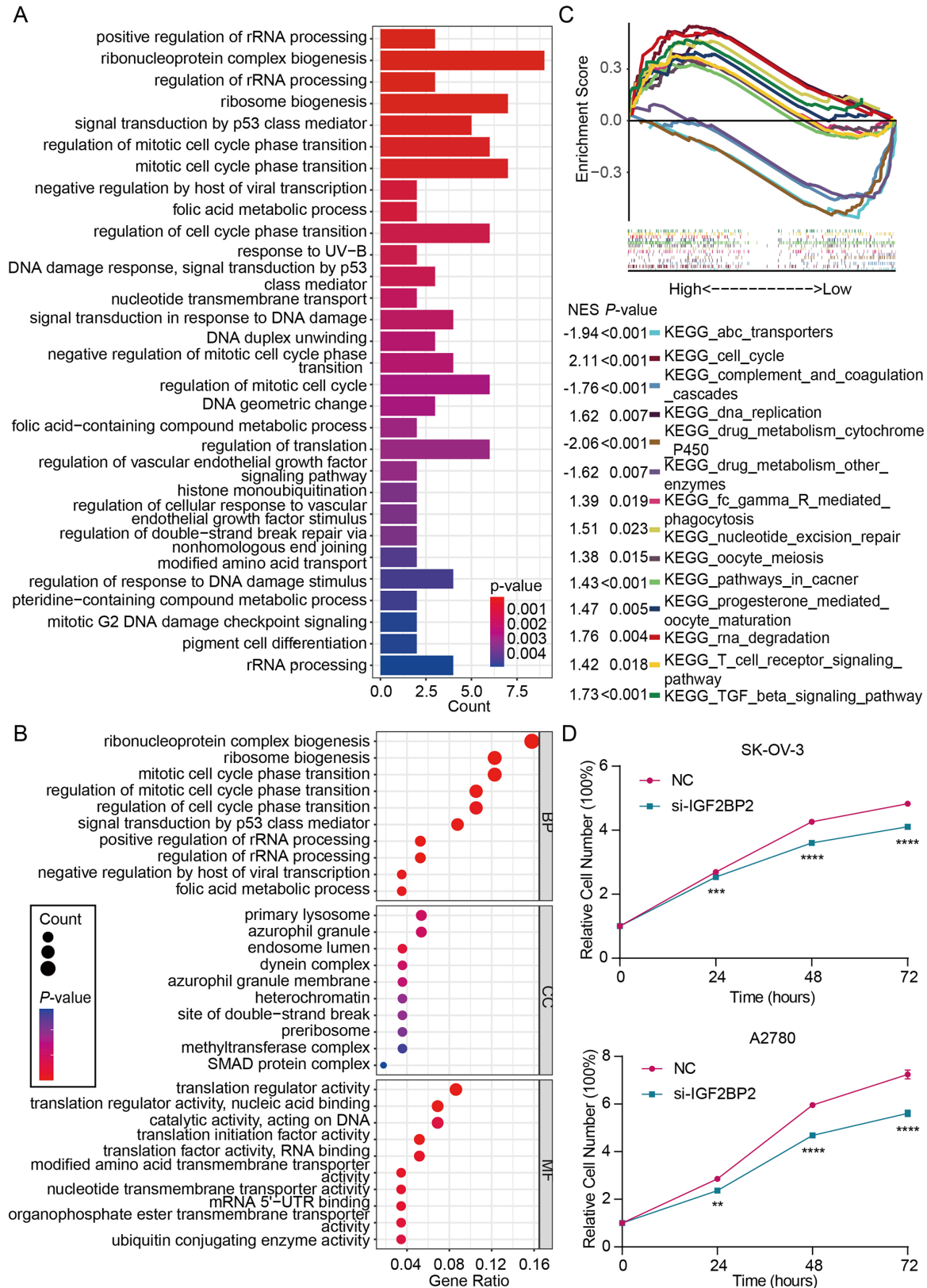


Figure 2. The functional analysis of IGF2BP2 in OC: (A) the top 30 pathways were obtained from Kyoto Encyclopedia of Genes and Genomes pathway enrichment analysis of intersecting genes positively or negatively associated with IGF2BP2; (B) functional enrichment analyses of these genes listed on the bubble plot contained the top 10 significant elements enriched in the Gene Ontology term categories: biological process, cellular component, and molecular function; (C) multi-gene set enrichment analysis of OC cell samples with high or low expression of IGF2BP2 obtained from Cancer Cell Line Encyclopedia. Each of these curves with a unique color represented one specific gene set with a significant P value less than 0.05; (D) detection of SK-OV-3 and A2780 cell proliferation after IGF2BP2 knockdown by the Cell Counting Kit-8 assay.

OC: ovarian cancer; IGF2BP2: insulin-like growth factor 2 mRNA-binding protein 2; IOSE: immortalized ovarian surface epithelial cells; NES: Normalized Enrichment Score.

P < 0.01; *P < 0.001; ****P < 0.0001.

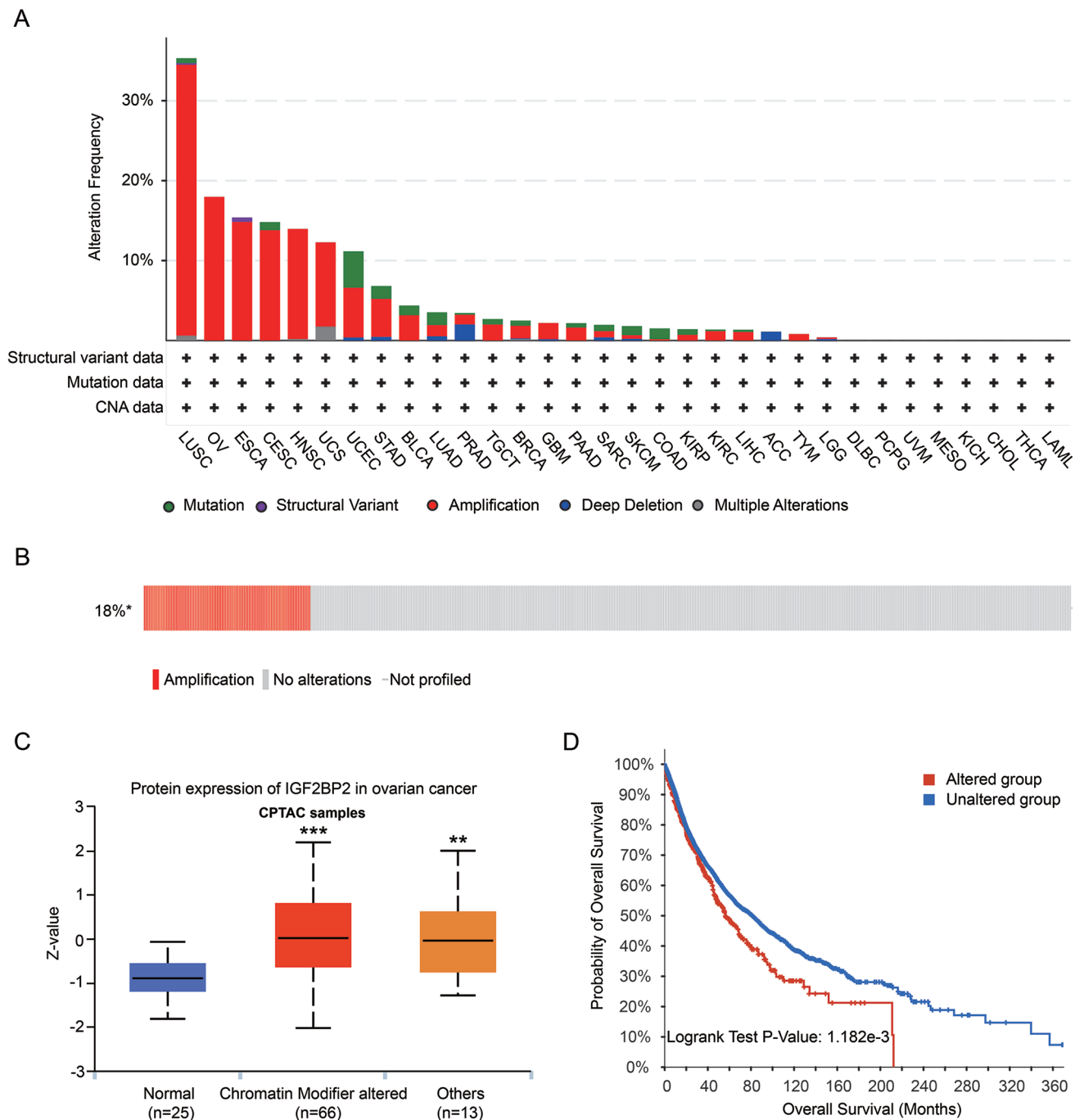


Figure 3. The genetic alterations of IGF2BP2: (A) alteration frequency of IGF2BP2 in TCGA pan-cancer data sets; (B) amplification of IGF2BP2 gene alteration in TCGA-OV by OncoPrint query; (C) the expression level of IGF2BP2 protein in the normal group, the chromatin modifier altered group, and others (DNA gene copy number alterations and gene mutation); (D) the overall survival of patients with ovarian cancer between the IGF2BP2 altered and unaltered groups by the Kaplan-Meier plotter.

IGF2BP2: insulin-like growth factor 2 mRNA-binding protein 2; TCGA: The Cancer Genome Atlas.

** $P < 0.01$; *** $P < 0.001$.

Discussion

This study proved that IGF2BP2 was overexpressed in OC and had oncogenic functions. The unfavorable survival of OC patients was found to be correlated with elevated IGF2BP2 expression. Furthermore, a positive correlation between IGF2BP2 expression and STAT1 expression and chemoresistance was observed. Moreover, IGF2BP2 expression was associated with TME and sensitivity to immunotherapy.

It has been shown that IGF2BP2 participates in a wide range of BPs and the dysregulation of IGF2BP2 leads to several metabolic diseases and cancers.⁵ Here, we demonstrated that IGF2BP2 was overexpressed in OC cells compared with non-tumorous ovarian cells. Indeed, an increase in IGF2BP2 expression has been observed in a series of cancers, including acute myeloid leukemia (AML),²⁰ breast cancer (BRCA),²¹ colorectal cancer (CRC),²² low-grade glioma (LGG),²³ hepatocellular carcinoma (HCC),²⁴ head and neck

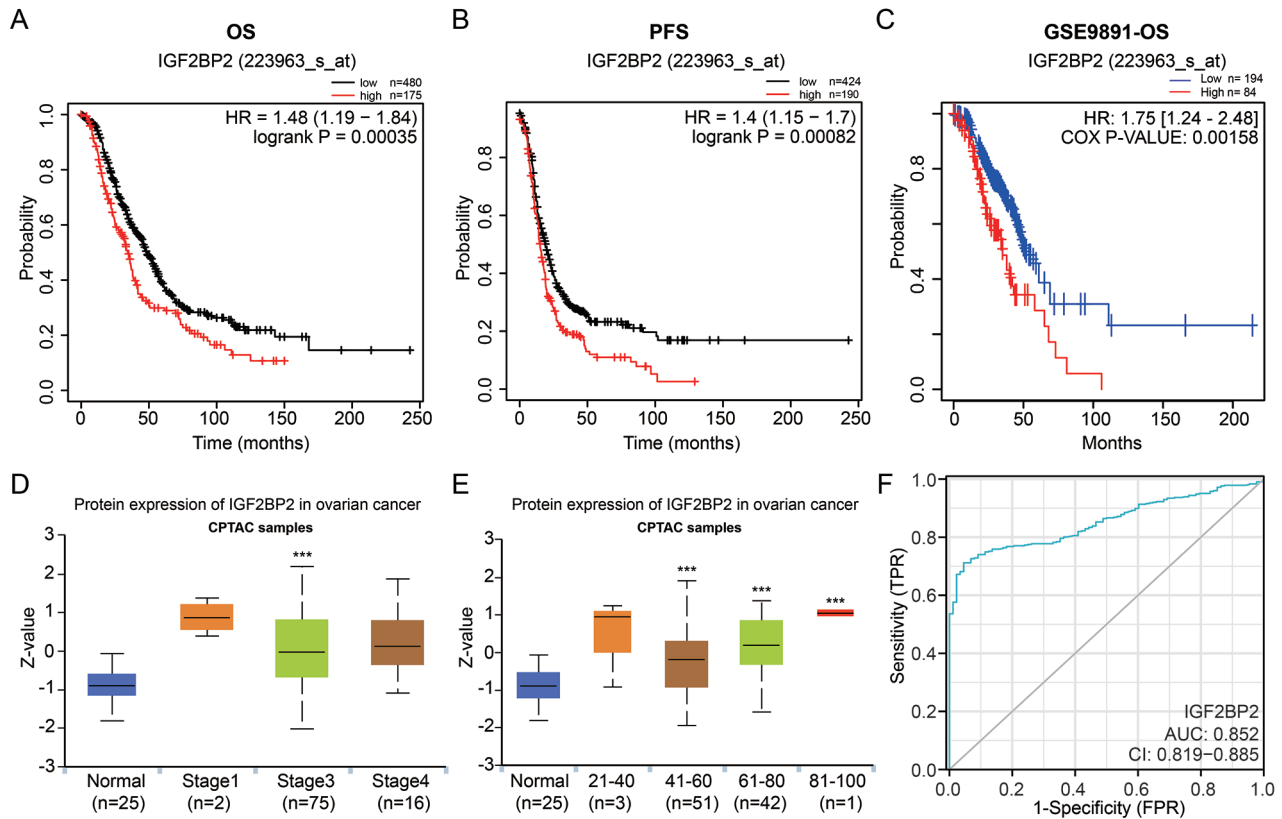


Figure 4. The prognosis value of IGF2BP2 in OC (OV): (A and B) analyses of OS and progression-free survival between the high expression and low expression of IGF2BP2 in OC; (C) survival curves showing the difference between IGF2BP2^{high} and IGF2BP2^{low} by analyzing the GSE9891 data set; (D and E) the association of IGF2BP2 protein expression with the tumor stages and ages of patients in Clinical Proteomic Tumor Analysis Consortium-OV; (F) receiver operating characteristic curve of IGF2BP2 in The Cancer Genome Atlas-OV.

IGF2BP2: insulin-like growth factor 2 mRNA-binding protein 2; TCGA: The Cancer Genome Atlas; TPR: true positive rate; FPR: false positive rate; OC: ovarian cancer; GSE: gene set enrichment.

*** $P < 0.001$ versus normal.

squamous cell carcinoma (HNSCC),²⁵ and pancreatic ductal adenocarcinoma (PDAC).⁶ These data indicate that IGF2BP2 may have a diagnostic value for patients with malignant tumors. Interestingly, the expression of IGF2BP2 protein was relatively higher in endometrioid OC cells (A2780) than in serous OC cells (OVCAR-3 and SK-OV-3), suggesting that the expression of IGF2BP2 may differ depending on their subtypes. It has been reported that IGF2BP2 has a significant effect on the regulation of the proliferation of SK-OV-3 and A2780 cells²⁶ and the chemoresistance of OC.²⁷ High expression of IGF2BP2 is related to unfavorable survival of OC patients.²⁸ This study demonstrated a remarkably high-expression level of IGF2BP2 in OC cells/tissues compared with non-tumorous ovarian epithelial cells/normal ovarian tissues, respectively, but was low in chemoresistant cells compared with chemosensitive cells. The high expression of IGF2BP2 was associated with low IC₅₀, indicating that cells with IGF2BP2 overexpression were sensitive to chemodrugs. This expression pattern was similar to the expression of STAT1 observed in our previous work.²⁹ By examination of the clinical data downloaded from UALCAN with statistical analysis, a positive correlation was found between Stage 3 and normal groups. In comparison with the normal group, the IGF2BP2 protein expression in OC patients at Stages 1 and 4 tended to be up-regulated but not significant. There was no Stage 2 data in the database. We speculated that at

the early stage of the disease, cancer cells with high IGF2BP2 are sensitive to chemotherapeutic agents such as PTX. After PTX treatment for a while, some OC cells die and others are transformed into resistant cells with a decrease in IGF2BP2 expression. Cancer stem cells also start to grow and differentiate, leading to chemoresistance.

This study showed that IGF2BP2 gene alteration in cancer was primarily distributed in the amplification of DNA gene copy number variations, predicting a worse prognosis. Furthermore, the gene alteration of IGF2BP2 in OC was in a large proportion, indicating that this chromatin modifier alteration might be a direct factor contributing to the high expression of IGF2BP2. DNA gene copy number variations are an essential factor for influencing gene expression and affect different BPs, and, therefore, account for the outcomes in cancer development and prognosis.³⁰ Indeed, somatic copy number alterations can predict response to platinum-based chemotherapy in OC.³¹ Therefore, IGF2BP2 would potentially be a predictive marker for OC prognosis and chemotherapy. Further validation may be needed in the large cohort study.

Interestingly, a positive correlation between IGF2BP2 expression and STAT1 expression was observed. Knockdown of IGF2BP2 decreased the expression of STAT1. Recently, the specific role of IGF2BP2 as an m⁶A regulatory factor controlling the expression of target transcripts in cancer has attracted extensive attention.⁵ Furthermore, overexpression

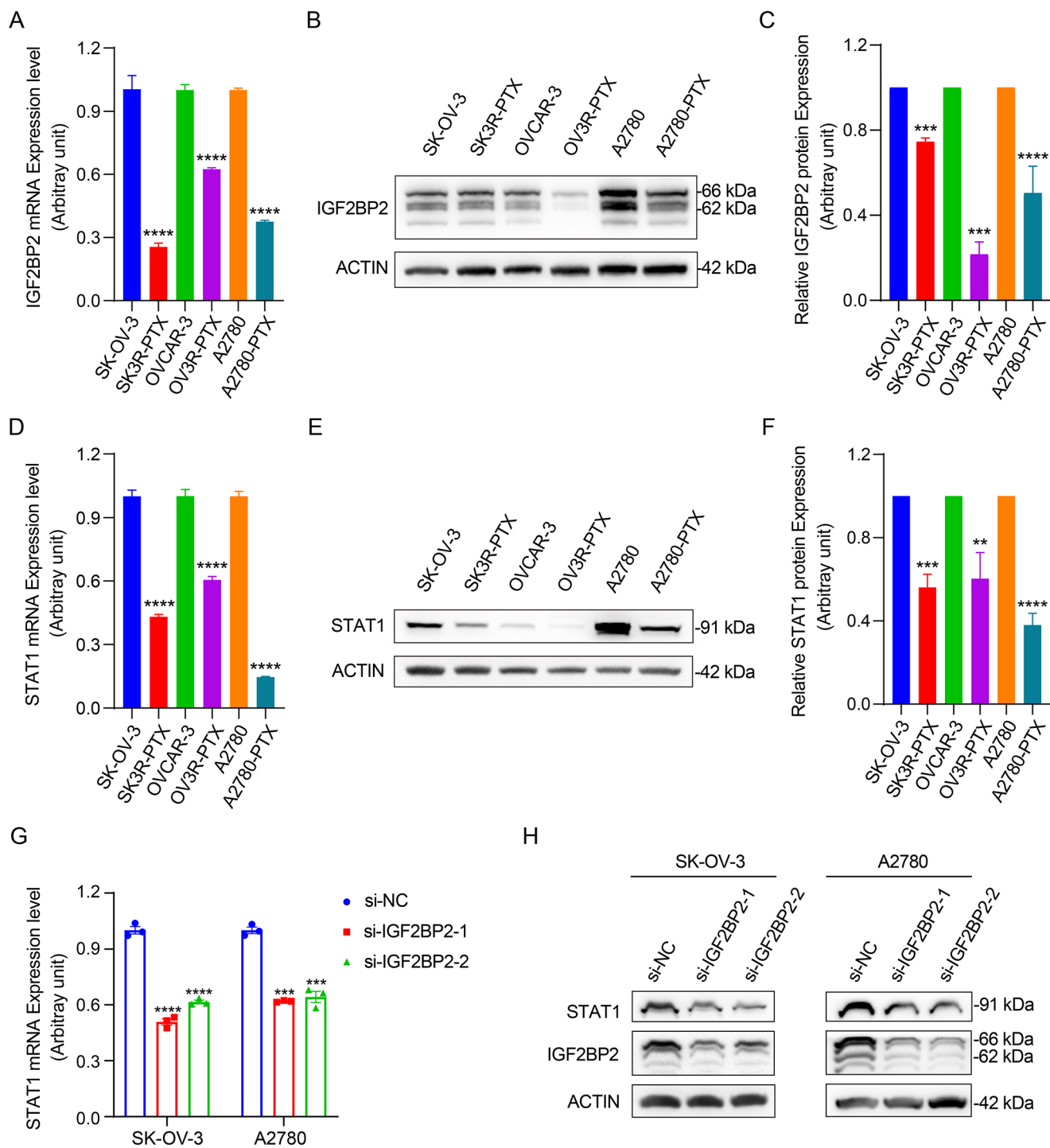


Figure 5. Association of IGF2BP2 with STAT1 and chemoresistant analyses: (A) detection of IGF2BP2 mRNA in OVCAR-3, SK-OV-3, and A2780 cells and their PTX-resistant counterparts OV3R-PTX, SK3R-PTX, and A2780-PTX cells by qRT-PCR ($n=3$); (B) detection of IGF2BP2 protein in OVCAR-3, SK-OV-3, A2780, OV3R-PTX, SK3R-PTX, and A2780-PTX cells by western blot. Representative images of IGF2BP2 and ACTIN are shown ($n=3$); (C) semi-quantitative analysis of the relative optical density of protein bands in (B) ($n=3$); (D) detection of STAT1 mRNA in OVCAR-3, SK-OV-3, A2780, OV3R-PTX, SK3R-PTX, and A2780-PTX cells by qRT-PCR ($n=3$); (E) detection of STAT1 protein in OVCAR-3, SK-OV-3, A2780, OV3R-PTX, SK3R-PTX, and A2780-PTX cells by western blot. Representative images of STAT1 and ACTIN are shown ($n=3$); (F) semi-quantitative analysis of the relative optical density of protein bands in (E) ($n=3$); (G and H) detection of STAT1 and IGF2BP2 expression at mRNA and protein levels after the knockdown of IGF2BP2 in ovarian cancer cell lines SK-OV-3 and A2780 by qRT-PCR ($n=3$) and western blot, in which representative images of STAT1, IGF2BP2, and ACTIN are shown ($n=2$).

STAT1: signal transducer and activator of transcription 1; PTX: paclitaxel; qRT-PCR: quantitative real-time polymerase chain reaction; IGF2BP2: insulin-like growth factor 2 mRNA-binding protein 2.

** $P < 0.01$; *** $P < 0.001$; **** $P < 0.0001$.

of IGF2BP2 resulted in an increase in STAT1 mRNA and protein expression. Our preliminary analysis of IGF2BP2 from the open-access database (<http://rm2target.canceromics.org/>), a comprehensive database for targets of RNA

methylation-related proteins, showed that IGF2BP2 was one of the binding m⁶A readers of STAT1 mRNA by RNA immunoprecipitation (RIP)-seq data analysis (GSE90639) in HEK293T cells,⁴ further supporting the IGF2BP2 associated

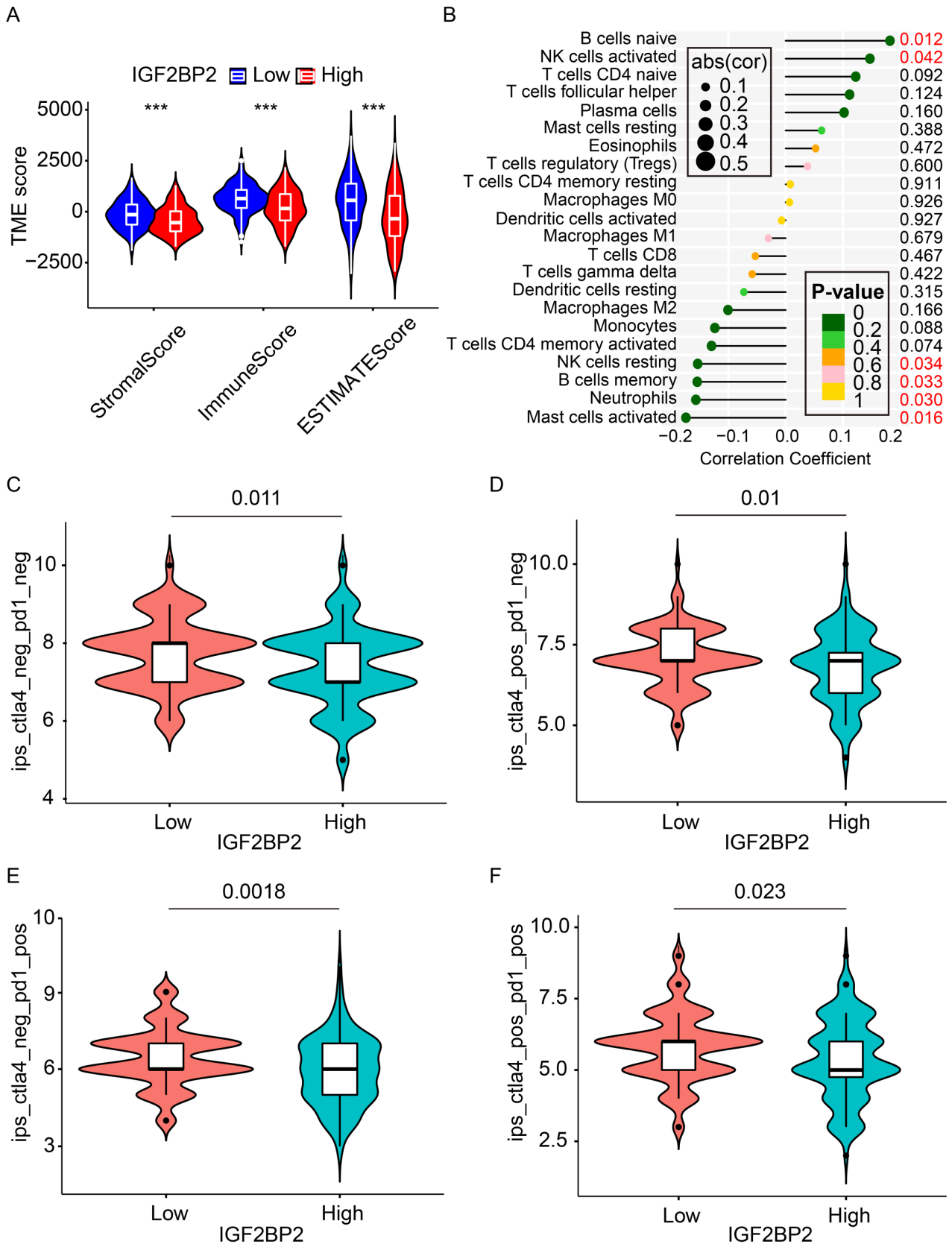


Figure 6. The expression correlation between IGF2BP2 and immunity: (A) the association of IGF2BP2 expression with tumor microenvironment scores (stroma, immune, and ESTIMATE) in TCGA-ovarian cancer patients. Scores were calculated by the ESTIMATE algorithm; (B) the lollipop figure showed the ratio of the differentiation of 22 types of tumor-infiltrating immune cells among the TCGA-OV samples with high and low IGF2BP2 expression. Red numbers indicate $P < 0.05$; (C to F) the expression of IGF2BP2 was associated with the sensitivity of immunotherapy (cytotoxic T-lymphocyte-associated protein 4 and programmed death-1 positive or negative). The number above the bar indicates a P value. IGF2BP2: insulin-like growth factor 2 mRNA-binding protein 2; TCGA: The Cancer Genome Atlas. *** $P < 0.001$.

STAT1 expression. High-expressed STAT1 may trigger the expression of PD-L1 to regulate immune cell infiltration in the TME.³² Our previous work demonstrated that STAT1 and PD-L1 were up-regulated in OC but down-regulated in PTX-resistant OC cells. However, there were no disparities of PD-1 expression between OC and normal control and between PTX-resistant and sensitive cells.¹¹ In the future, we need more clinical data to analyze and more validation to explore the interaction mechanism between IGF2BP2 and STAT1 in OC chemotherapy and immunotherapy. Bioinformatics analysis of drug sensitivity showed that compared with the high expression of IGF2BP2, patients with low expression of IGF2BP2 were less sensitive to chemotherapeutic agents. Interestingly, in the prediction of immunotherapeutic sensitivity, patients with low expression of IGF2BP2 were more sensitive to the immune checkpoint inhibitors (anti-CTLA4 and anti-PD-1) compared with patients with high expression of IGF2BP2. It has been shown that the knockdown of IGF2BP2 inhibits PD-L1 expression in hypopharyngeal carcinoma cells and the interaction between IGF2BP2 and PD-L1 RNA is validated by RNA pull-down assays.³³ These data suggest that high expression of IGF2BP2 favored the chemotherapy but low expression of IGF2BP2 was beneficial to the immunotherapy. Our findings showed that IGF2BP2 expression was higher in OC cells but lower in PTX-resistant cells, implying that IGF2BP2 may be a key molecule involved in chemotherapy and immunotherapy. Indeed, it has been reported that IGF2BP2 interaction with circITGB6 can facilitate the stability of FGF9 mRNA, leading to the shift of macrophages toward the M2 phenotype in the TME in cisplatin-resistant OC.³⁴ IGF2BP2 can enhance the stability of lncRNA-AC026356.1 in lung cancer A549-cisplatin cells, whereas lncRNA-AC026356.1 positively correlates with immune cells such as Th1 and Tem cells and negatively correlates with T-cell exhaustion.³⁵ Recently, the remarkable advancements of immunotherapy have made revolutionary changes in the treatment of cancer because of the understanding of the characteristics of the immune microenvironment. Therefore, immune checkpoint inhibitors, including CTLA-4 and its ligand B7/CD8, and PD-1 and its ligand PD-L1,³⁶ may apply to cancer patients. Previous reports show that the combining therapy of anti-PD-1 and anti-CTLA-4 antibodies results in distinct immunologic changes³⁷ and is potentially used in OC.³⁸ Our study explored, for the first time, the responsibility and function of IGF2BP2 in OC chemotherapy and immunotherapy.

The CIBERSORT analysis of this study revealed a remarkable association between IGF2BP2 expression and TICs. In the TME, activated mast cells could exacerbate tumor immune suppression by releasing adenosine and increasing T-regulatory cells, thereby enhancing the suppression of T cells and NK cells in tumors.³⁹ These data suggest that the suppression of IGF2BP2 expression would reduce mast cell activation. The tumor-associated macrophages (TAMs) may also play an immunosuppressive role in the TME of high-grade serous OC.⁴⁰ The neutrophils exhibited plasticity and could be polarized into antitumor (N1) or pro-tumor (N2) phenotypes depending on environmental factors⁴¹ but the specific role of neutrophils in OC remains to be explored. Furthermore, B cells and NK cells have been reported to exhibit beneficial impacts on antitumor immunity.^{29,42} Our study demonstrated

that IGF2BP2 expression was positively correlated with the B-cell naive and NK cells activated, but negatively correlated with the B-cell memory and NK cells resting. Therefore, the significant relationship between TICs and IGF2BP2 expression implies the importance of IGF2BP2 in antitumor immunity and the tumor microenvironment.

Conclusions

Overexpression and genomic alteration of IGF2BP2 are found in OC cells. Knockdown of IGF2BP2 inhibits OC cell proliferation. High-expressed IGF2BP2 is correlated with STAT1 expression and unfavorable prognosis of OC patients. After PTX treatment for a while, some cancer cells died but resistant cells survived. The alteration of IGF2BP2 expression may respond to chemotherapy and immunotherapy, and IGF2BP2 shows potential as a therapeutic target and diagnostic biomarker for OC.

AUTHORS' CONTRIBUTIONS

All authors participated in the design, interpretation of the studies, analysis of the data, and review of the article. JY conducted the experiments, performed the bioinformatics analysis, analyzed data, and wrote the draft of the article. XL performed partial experiments and bioinformatics analysis. FW and HL validated and analyzed data. WG provided experimental in part. GX did supervision, conceptualization, project administration, and wrote and edited the final article. All authors contributed to the article and approved the submitted version.

DECLARATION OF CONFLICTING INTERESTS

The author(s) declared no potential conflicts of interest with respect to the research, authorship, and/or publication of this article.

FUNDING

The author(s) disclosed receipt of the following financial support for the research, authorship, and/or publication of this article: This work was supported by the National Natural Science Foundation of China (grant no. 81872121), and the Science and Technology Commission of Shanghai Municipality (grant no. 23ZR1408900).

ORCID ID

Guoxiong Xu  <https://orcid.org/0000-0002-9074-8754>

SUPPLEMENTAL MATERIAL

Supplemental material for this article is available online.

REFERENCES

1. Siegel RL, Miller KD, Fuchs HE, Jemal A. Cancer statistics, 2022. *CA Cancer J Clin* 2022;72:7–33
2. Banerjee S, Kaye SB. New strategies in the treatment of ovarian cancer: current clinical perspectives and future potential. *Clin Cancer Res* 2013;19:961–8
3. Buechel M, Herzog TJ, Westin SN, Coleman RL, Monk BJ, Moore KN. Treatment of patients with recurrent epithelial ovarian cancer for whom platinum is still an option. *Ann Oncol* 2019;30:721–32
4. Huang H, Weng H, Sun W, Qin X, Shi H, Wu H, Zhao BS, Mesquita A, Liu C, Yuan CL, Hu YC, Huttelmaier S, Skibbe JR, Su R, Deng X, Dong L, Sun M, Li C, Nachtergaele S, Wang Y, Hu C, Ferchen K, Greis KD, Jiang X, Wei M, Qu L, Guan JL, He C, Yang J, Chen J. Recognition

- of RNA N(6)-methyladenosine by IGF2BP proteins enhances mRNA stability and translation. *Nat Cell Biol* 2018;**20**:285–95
5. Wang J, Chen L, Qiang P. The role of IGF2BP2, an m6A reader gene, in human metabolic diseases and cancers. *Cancer Cell Int* 2021;**21**:99
 6. Dahlem C, Barghash A, Puchas P, Haybaeck J, Kessler SM. The insulin-like growth factor 2 mRNA binding protein IMP2/IGF2BP2 is over-expressed and correlates with poor survival in pancreatic cancer. *Int J Mol Sci* 2019;**20**:3204
 7. Wang S, Li Z, Zhu G, Hong L, Hu C, Wang K, Cui K, Hao C. RNA-binding protein IGF2BP2 enhances circ_0000745 abundance and promotes aggressiveness and stemness of ovarian cancer cells via the microRNA-3187-3p/ERBB4/PI3K/AKT axis. *J Ovarian Res* 2021;**14**:154
 8. Tian X, Guan W, Zhang L, Sun W, Zhou D, Lin Q, Ren W, Nadeem L, Xu G. Physical interaction of STAT1 isoforms with TGF-beta receptors leads to functional crosstalk between two signaling pathways in epithelial ovarian cancer. *J Exp Clin Cancer Res* 2018;**37**:103
 9. Wang F, Zhang L, Liu J, Zhang J, Xu G. Highly expressed STAT1 contributes to the suppression of stemness properties in human paclitaxel-resistant ovarian cancer cells. *Aging (Albany NY)* 2020;**12**:11042–60
 10. Wang T, Kong S, Tao M, Ju S. The potential role of RNA N6-methyladenosine in Cancer progression. *Mol Cancer* 2020;**19**:88
 11. Liu F, Liu J, Zhang J, Shi J, Gui L, Xu G. Expression of STAT1 is positively correlated with PD-L1 in human ovarian cancer. *Cancer Biol Ther* 2020;**21**:963–71
 12. Zhang J, Guan W, Xu X, Wang F, Li X, Xu G. A novel homeostatic loop of sorcin drives paclitaxel-resistance and malignant progression via Smad4/ZEB1/miR-142-5p in human ovarian cancer. *Oncogene* 2021;**40**:4906–18
 13. Mizuno H, Kitada K, Nakai K, Sarai A. PrognoScan: a new database for meta-analysis of the prognostic value of genes. *BMC Med Genomics* 2009;**2**:18
 14. Chandrashekar DS, Bashel B, Balasubramanya SAH, Creighton CJ, Ponce-Rodriguez I, Chakravarthi BVS, Varambally S. UALCAN: a portal for facilitating tumor subgroup gene expression and survival analyses. *Neoplasia* 2017;**19**:649–58
 15. Fluss R, Faraggi D, Reiser B. Estimation of the Youden Index and its associated cutoff point. *Biom J* 2005;**47**:458–72
 16. Gao J, Aksoy BA, Dogrusoz U, Dresdner G, Gross B, Sumer SO, Sun Y, Jacobsen A, Sinha R, Larsson E, Cerami E, Sander C, Schultz N. Integrative analysis of complex cancer genomics and clinical profiles using the cBioPortal. *Sci Signal* 2013;**6**:pl1
 17. Gleeleher P, Cox N, Huang RS. pRRophetic: an R package for prediction of clinical chemotherapeutic response from tumor gene expression levels. *PLoS ONE* 2014;**9**:e107468
 18. Yoshihara K, Shahmoradgoli M, Martínez E, Vegesna R, Kim H, Torres-Garcia W, Treviño V, Shen H, Laird PW, Levine DA, Carter SL, Getz G, Stenke-Hale K, Mills GB, Verhaak RG. Inferring tumour purity and stromal and immune cell admixture from expression data. *Nat Commun* 2013;**4**:2612
 19. Newman AM, Liu CL, Green MR, Gentles AJ, Feng W, Xu Y, Hoang CD, Diehn M, Alizadeh AA. Robust enumeration of cell subsets from tissue expression profiles. *Nat Methods* 2015;**12**:453–7
 20. He X, Li W, Liang X, Zhu X, Zhang L, Huang Y, Yu T, Li S, Chen Z. IGF2BP2 overexpression indicates poor survival in patients with acute myelocytic leukemia. *Cell Physiol Biochem* 2018;**51**:1945–56
 21. Barghash A, Helms V, Kessler SM. Overexpression of IGF2 mRNA-binding protein 2 (IMP2/p62) as a feature of basal-like breast cancer correlates with short survival. *Scand J Immunol* 2015;**82**:142–3
 22. Cui J, Tian J, Wang W, He T, Li X, Gu C, Wang L, Wu J, Shang A. IGF2BP2 promotes the progression of colorectal cancer through a YAP-dependent mechanism. *Cancer Sci* 2021;**112**:4087–99
 23. Yang Y, Liu X, Cheng L, Li L, Wei Z, Wang Z, Han G, Wan X, Wang Z, Zhang J, Chen C. Tumor suppressor microRNA-138 suppresses low-grade glioma development and metastasis via regulating IGF2BP2. *Onco Targets Ther* 2020;**13**:2247–60
 24. Kessler SM, Laggai S, Barghash A, Schultheiss CS, Lederer E, Arlt M, Helms V, Haybaeck J, Kiemer AK. IMP2/p62 induces genomic instability and an aggressive hepatocellular carcinoma phenotype. *Cell Death Dis* 2015;**6**:e1894
 25. Yu D, Pan M, Li Y, Lu T, Wang Z, Liu C, Hu G. RNA N6-methyladenosine reader IGF2BP2 promotes lymphatic metastasis and epithelial-mesenchymal transition of head and neck squamous carcinoma cells via stabilizing slug mRNA in an m6A-dependent manner. *J Exp Clin Cancer Res* 2022;**41**:6
 26. Ji J, Li C, Wang J, Wang L, Huang H, Li Y, Fang J. Hsa_circ_0001756 promotes ovarian cancer progression through regulating IGF2BP2-mediated RAB5A expression and the EGFR/MAPK signaling pathway. *Cell Cycle* 2022;**21**:685–96
 27. Fu L, Zhang D, Yi N, Cao Y, Wei Y, Wang W, Li L. Circular RNA circ-cPBX3 promotes cisplatin resistance of ovarian cancer cells via interacting with IGF2BP2 to stabilize ATP7A mRNA expression. *Hum Cell* 2022;**35**:1560–76
 28. Sekulovski N, MacLean JA, Bheemireddy SR, Yu Z, Okuda H, Pru C, Plunkett KN, Matzuk M, Hayashi K. Niclosamide's potential direct targets in ovarian cancer. *Biol Reprod* 2021;**105**:403–12
 29. Sharonov GV, Serebrovskaya EO, Yuzhakova DV, Britanova OV, Chudakov DM. B cells, plasma cells and antibody repertoires in the tumour microenvironment. *Nat Rev Immunol* 2020;**20**:294–307
 30. Liang L, Fang JY, Xu J. Gastric cancer and gene copy number variation: emerging cancer drivers for targeted therapy. *Oncogene* 2016;**35**:1475–82
 31. Despierre E, Moisse M, Yesilyurt B, Sehoul J, Braicu I, Mahner S, Castillo-Tong DC, Zeillinger R, Lambrechts S, Leunen K, Amant F, Moerman P, Lambrechts D, Vergote I. Somatic copy number alterations predict response to platinum therapy in epithelial ovarian cancer. *Gynecol Oncol* 2014;**135**:415–22
 32. El-Arabey AA, Abdalla M, Abd-Allah AR. SnapShot: TP53 status and macrophages infiltration in TCGA-analyzed tumors. *Int Immunopharmacol* 2020;**86**:106758
 33. Yang X, Liu J. Targeting PD-L1 (programmed death-ligand 1) and inhibiting the expression of IGF2BP2 (insulin-like growth factor 2 mRNA-binding protein 2) affect the proliferation and apoptosis of hypopharyngeal carcinoma cells. *Bioengineered* 2021;**12**:7755–64
 34. Li H, Luo F, Jiang X, Zhang W, Xiang T, Pan Q, Cai L, Zhao J, Weng D, Li Y, Dai Y, Sun F, Yang C, Huang Y, Yang J, Tang Y, Han Y, He M, Zhang Y, Song L, Xia JC. CircITGB6 promotes ovarian cancer cisplatin resistance by resetting tumor-associated macrophage polarization toward the M2 phenotype. *J Immunother Cancer* 2022;**10**:e004029
 35. Zhang Z, Tan X, Wu R, Deng T, Wang H, Jiang X, Zeng P, Tang J. m6A-mediated upregulation of lncRNA-AC026356.1 promotes cancer stem cell maintenance in lung adenocarcinoma via activating Wnt signaling pathway. *Aging (Albany NY)* 2023;**15**:3538–48
 36. Buchbinder EI, Desai A. CTLA-4 and PD-1 pathways: similarities, differences, and implications of their inhibition. *Am J Clin Oncol* 2016;**39**:98–106
 37. Das R, Verma R, Szoln M, Boddupalli CS, Gettinger SN, Kluger H, Callahan M, Wolchok JD, Halaban R, Dhodapkar MV, Dhodapkar KM. Combination therapy with anti-CTLA-4 and anti-PD-1 leads to distinct immunologic changes in vivo. *J Immunol* 2015;**194**:950–9
 38. Farghaly SA. Combination therapy of cytotoxic t-lymphocyte-associated antigen 4 (CTLA-4) and programmed death 1 (PD 1) blocker, check point inhibitors for treatment of patients with advanced and recurrent epithelial ovarian cancer. *Eur J Gynaecol Oncol* 2017;**38**:7–9
 39. Huang B, Lei Z, Zhang GM, Li D, Song C, Li B, Liu Y, Yuan Y, Unkeless J, Xiong H, Feng ZH. SCF-mediated mast cell infiltration and activation exacerbate the inflammation and immunosuppression in tumor microenvironment. *Blood* 2008;**112**:1269–79
 40. El-Arabey AA, Denizli M, Kanlikilicer P, Bayraktar R, Ivan C, Rashed M, Kabil N, Ozpolat B, Calin GA, Salama SA, Abd-Allah AR, Sood AK, Lopez-Berestein G. GATA3 as a master regulator for interactions of tumor-associated macrophages with high-grade serous ovarian carcinoma. *Cell Signal* 2020;**68**:109539
 41. Fridlender ZG, Sun J, Kim S, Kapoor V, Cheng G, Ling L, Worthen GS, Albelda SM. Polarization of tumor-associated neutrophil phenotype by TGF-beta: "N1" versus "N2" TAN. *Cancer Cell* 2009;**16**:183–94
 42. Cozar B, Greppi M, Carpentier S, Narni-Mancinelli E, Chiosso L, Vivier E. Tumor-infiltrating natural killer cells. *Cancer Discov* 2021;**11**:34–44